


Cross sections for inelastic $K+\phi$ scattering*

Yi-Hao Pan (潘奕豪) Xiao-Ming Xu (许晓明)[†] 

Department of Physics, Shanghai University, Baoshan, Shanghai 200444, China

Abstract: In the first Born approximation, we study the reactions $K\phi \rightarrow \pi K$, ρK , πK^* , and ρK^* with quark-anti-quark annihilation and creation. Transition amplitudes are derived with the development in the spherical harmonics of the relative-motion wave functions of two initial mesons and two final mesons so that parity is conserved and the total angular momentum of the final mesons equals that of the initial mesons. Unpolarized cross sections are calculated from the transition amplitudes that also contain mesonic quark-antiquark relative-motion wave functions and transition potentials for quark-antiquark annihilation and creation. The notable temperature dependence of the cross sections is shown. The cross sections for $K\phi \rightarrow \rho K$, $K\phi \rightarrow \pi K^*$, and $K\phi \rightarrow \rho K^*$ may be of the millibarn scale, whereas the cross section for $K\phi \rightarrow \pi K$ is small.

Keywords: meson-meson scattering, quark-antiquark annihilation and creation, quark potential model

DOI: 10.1088/1674-1137/acd9be

I. INTRODUCTION

Since enhanced ϕ yield was first suggested as a signature for the formation of quark-gluon plasmas [1, 2], many measurements on ϕ mesons have been made in relativistic heavy-ion collisions, such as Au-Au collisions at the BNL Relativistic Heavy Ion Collider [3–11] and Pb-Pb collisions at the CERN Large Hadron Collider [12–15]. Measured ratios such as ϕ/π , ϕ/K , and Ω/ϕ exhibit enhancement in ϕ mesons produced in relativistic heavy-ion collisions relative to $p+p$ collisions. This indicates that strange quarks and strange antiquarks are produced in parton-parton scattering in initial nucleus-nucleus collisions and deconfined matter. The combination of a strange quark and strange antiquark forms a ϕ meson at the hadronization of quark-gluon plasma. The ϕ meson in collisions with hadrons in hadronic matter may be broken, and this changes the ϕ yield. For example, the ϕ nuclear modification factor as a function of transverse momentum is smaller than 1 for central and midcentral Au-Au collisions at the center-of-mass energy per nucleon-nucleon pair $\sqrt{s_{NN}} = 200$ GeV [3, 6] and for central and midcentral Pb-Pb collisions at $\sqrt{s_{NN}} = 2.76$ TeV [13]. Therefore, studying inelastic hadron- ϕ scattering is fundamental in relativistic heavy-ion collisions.

Hadron- ϕ reactions can be studied in hadron degrees of freedom [16–22] or quark degrees of freedom [23, 24]. Starting from an effective meson Lagrangian, Feynman diagrams with one-kaon exchange have been considered,

and squared invariant amplitudes for $\pi\phi \rightarrow K\bar{K}^* + K^*\bar{K}$, $\rho\phi \rightarrow K\bar{K}$, and $\phi\phi \rightarrow K\bar{K}$ were provided in Ref. [17]. By using a Lagrangian based on an effective theory in which vector mesons are identified as the dynamical gauge bosons of the hidden $U(3)_V$ local symmetry in the $U(3)_L \times U(3)_R / U(3)_V$ nonlinear sigma model, large cross sections for $K^*\phi \rightarrow \pi K$ and $K\phi \rightarrow \pi K^*$ were obtained in Ref. [22]. With $\pi\phi\rho$ coupling, cross sections for $\phi N \rightarrow \pi N$, $\phi N \rightarrow \rho N$, and $\phi N \rightarrow \pi\Delta$ were obtained in Ref. [20]. With $N\Lambda K$ coupling, cross sections for $\phi N \rightarrow K\Lambda$ were shown to be considerably larger than those for $\phi N \rightarrow \pi N$, $\phi N \rightarrow \rho N$, and $\phi N \rightarrow \pi\Delta$. Experimental efforts to extract the $\phi + N$ total cross section from $d(\gamma, pK^+K^-)n$ have been made by the CLAS Collaboration [25]. The $\phi + N$ cross section may lead to a difference in ϕ production between π^- -induced reactions on C and W targets [26]. Inelastic $\pi + \phi$ scattering and inelastic $\rho + \phi$ scattering were studied in Ref. [23] in the quark interchange mechanism [27, 28]. By adopting temperature dependence in a quark potential, mesonic quark-antiquark wave functions, and meson masses, prominent temperature-dependent cross sections were obtained for inelastic $\pi + \phi$ and $\rho + \phi$ scattering in hadronic matter [23]. Besides pions and rho mesons, kaons in hadronic matter also interact with ϕ mesons. However, the quark-level study of inelastic $K + \phi$ scattering has not yet been conducted. Moreover, the temperature dependence of inelastic $K + \phi$ scattering is unexplored both experimentally and theoretically. Therefore, this study aims to investigate inelastic

Received 11 March 2023; Accepted 29 May 2023; Published online 30 May 2023

* Supported by the National Natural Science Foundation of China (11175111)

[†] E-mail: xmxu@mail.shu.edu.cn

©2023 Chinese Physical Society and the Institute of High Energy Physics of the Chinese Academy of Sciences and the Institute of Modern Physics of the Chinese Academy of Sciences and IOP Publishing Ltd

$K + \phi$ scattering and its temperature dependence.

Some meson-meson reactions may be dominated by the process of a quark and an antiquark annihilating into a gluon, followed by the gluon creating another quark-antiquark pair. Such quark-antiquark annihilation and creation has been used in Refs. [29, 30] to obtain unpolarized cross sections for the reactions $\pi\pi \rightarrow \rho\rho$, $K\bar{K} \rightarrow K^*\bar{K}^*$, $K\bar{K}^* \rightarrow K^*\bar{K}$, $K^*\bar{K} \rightarrow K^*\bar{K}^*$, $\pi\pi \rightarrow K\bar{K}$, $\pi\rho \rightarrow K\bar{K}^*$, $\pi\rho \rightarrow K^*\bar{K}$, $K\bar{K} \rightarrow \rho\rho$, $K\bar{K} \rightarrow K\bar{K}^*$, $K\bar{K} \rightarrow K^*\bar{K}$, $\pi K \rightarrow \pi K^*$, $\pi K \rightarrow \rho K$, $\pi\pi \rightarrow K\bar{K}^*$, $\pi\pi \rightarrow K^*\bar{K}$, $\pi\pi \rightarrow K^*\bar{K}^*$, $\pi\rho \rightarrow K\bar{K}$, $\pi\rho \rightarrow K^*\bar{K}^*$, $\rho\rho \rightarrow K^*\bar{K}^*$, $K\bar{K}^* \rightarrow \rho\rho$ and $K^*\bar{K} \rightarrow \rho\rho$. The s quark (or \bar{s} antiquark) of a kaon may annihilate with the \bar{s} antiquark (or s quark) of a ϕ meson to produce a gluon, and subsequently, the gluon splits into a $u\bar{u}$ or $d\bar{d}$ pair. The $u\bar{u}$ or $d\bar{d}$ pair combines with spectator constituents of the K and ϕ mesons to form two mesons that are not ϕ mesons. Thus, quark-antiquark annihilation and creation leads to inelastic $K + \phi$ scattering. By contrast, quark interchange does not cause inelastic $K + \phi$ scattering. The mechanism that governs inelastic $K + \phi$ scattering completely differs from the mechanism that governs inelastic $\pi + \phi$ and $\rho + \phi$ scattering. Therefore, with quark-antiquark annihilation and creation in the first Born approximation, we study the reactions $K\phi \rightarrow \pi K$, $K\phi \rightarrow \rho K$, $K\phi \rightarrow \pi K^*$, and $K\phi \rightarrow \rho K^*$.

The remainder of this paper is organized as follows. In the next section, we derive transition-amplitude formulas for 2-to-2 meson-meson scattering driven by quark-antiquark annihilation and creation. Numerical results and relevant discussions are given in Sec. III. A summary is presented in the final section.

II. FORMALISM

The reaction $A(q_1\bar{q}_1) + B(q_2\bar{q}_2) \rightarrow C(q_3\bar{q}_1) + D(q_2\bar{q}_4)$ ($A(q_1\bar{q}_1) + B(q_2\bar{q}_2) \rightarrow C(q_1\bar{q}_4) + D(q_3\bar{q}_2)$) takes place when a quark q_1 (q_2) and antiquark \bar{q}_2 (\bar{q}_1) in the initial mesons annihilate into a gluon, and the gluon subsequently creates a quark q_3 and antiquark \bar{q}_4 . The two processes $q_1 + \bar{q}_2 \rightarrow q_3 + \bar{q}_4$ and $\bar{q}_1 + q_2 \rightarrow q_3 + \bar{q}_4$ give rise to the two transition potentials $V_{aq_1\bar{q}_2}$ and $V_{a\bar{q}_1q_2}$, respectively. E_i and \vec{P}_i (E_f and \vec{P}_f) denote the total energy and total momentum of the two initial (final) mesons, respectively. Let E_A (E_B , E_C , E_D) be the energy of meson A (B , C , D), and V the volume where every meson wave function is normalized. The S -matrix element for $A + B \rightarrow C + D$ is

$$S_{fi} = \delta_{fi} - (2\pi)^4 i\delta(E_f - E_i)\delta^3(\vec{P}_f - \vec{P}_i) \frac{M_{aq_1\bar{q}_2} + M_{a\bar{q}_1q_2}}{V^2 \sqrt{2E_A 2E_B 2E_C 2E_D}}, \quad (1)$$

where $M_{aq_1\bar{q}_2}$ and $M_{a\bar{q}_1q_2}$ are the transition amplitudes given by

$$\begin{aligned} M_{aq_1\bar{q}_2} &= \frac{(m_{q_3} + m_{\bar{q}_4})^3}{m_{q_1}^3} \sqrt{2E_A 2E_B 2E_C 2E_D} \\ &\times \int d\vec{r}_{q_1\bar{q}_1} d\vec{r}_{q_2\bar{q}_2} d\vec{r}_{q_3\bar{q}_1, q_2\bar{q}_4} \psi_{CD}^+ V_{aq_1\bar{q}_2} \\ &\times \psi_{AB} e^{i\vec{p}_{q_1\bar{q}_1, q_2\bar{q}_2} \cdot \vec{r}_{q_1\bar{q}_1, q_2\bar{q}_2} - i\vec{p}_{q_3\bar{q}_1, q_2\bar{q}_4} \cdot \vec{r}_{q_3\bar{q}_1, q_2\bar{q}_4}}, \end{aligned} \quad (2)$$

$$\begin{aligned} M_{a\bar{q}_1q_2} &= \frac{(m_{q_1} + m_{\bar{q}_4})^3}{m_{q_1}^3} \sqrt{2E_A 2E_B 2E_C 2E_D} \\ &\times \int d\vec{r}_{q_1\bar{q}_1} d\vec{r}_{q_3\bar{q}_2} d\vec{r}_{q_1\bar{q}_4, q_3\bar{q}_2} \psi_{CD}^+ V_{a\bar{q}_1q_2} \\ &\times \psi_{AB} e^{i\vec{p}_{q_1\bar{q}_1, q_2\bar{q}_2} \cdot \vec{r}_{q_1\bar{q}_1, q_2\bar{q}_2} - i\vec{p}_{q_1\bar{q}_4, q_3\bar{q}_2} \cdot \vec{r}_{q_1\bar{q}_4, q_3\bar{q}_2}}, \end{aligned} \quad (3)$$

where m_{q_1} ($m_{\bar{q}_1}$, m_{q_3} , $m_{\bar{q}_4}$) is the mass of q_1 (\bar{q}_1 , q_3 , \bar{q}_4), \vec{r}_{ab} is the relative coordinate of constituents a and b , $\vec{r}_{q_1\bar{q}_1, q_2\bar{q}_2}$ ($\vec{r}_{q_3\bar{q}_1, q_2\bar{q}_4}$, $\vec{r}_{q_1\bar{q}_4, q_3\bar{q}_2}$) is the relative coordinate of $q_1\bar{q}_1$ and $q_2\bar{q}_2$ ($q_3\bar{q}_1$ and $q_2\bar{q}_4$, $q_1\bar{q}_4$ and $q_3\bar{q}_2$), $\vec{p}_{q_1\bar{q}_1, q_2\bar{q}_2}$ ($\vec{p}_{q_3\bar{q}_1, q_2\bar{q}_4}$, $\vec{p}_{q_1\bar{q}_4, q_3\bar{q}_2}$) is the relative momentum of $q_1\bar{q}_1$ and $q_2\bar{q}_2$ ($q_3\bar{q}_1$ and $q_2\bar{q}_4$, $q_1\bar{q}_4$ and $q_3\bar{q}_2$), ψ_{AB} (ψ_{CD}) is the wave function of mesons A and B (C and D), and ψ_{AB}^+ (ψ_{CD}^+) is the Hermitian conjugate of ψ_{AB} (ψ_{CD}). The wave function of mesons A and B is

$$\psi_{AB} = \phi_{Acolor} \phi_{Bcolor} \phi_{Arel} \phi_{Brel} \chi_{S_A S_{A_z}} \chi_{S_B S_{B_z}} \varphi_{ABflavor}, \quad (4)$$

and the wave function of mesons C and D is

$$\psi_{CD} = \phi_{Ccolor} \phi_{Dcolor} \phi_{Crel} \phi_{Drel} \chi_{S_C S_{C_z}} \chi_{S_D S_{D_z}} \varphi_{CDflavor}, \quad (5)$$

where S_A (S_B , S_C , S_D) is the spin of meson A (B , C , D) with its magnetic projection quantum number S_{A_z} (S_{B_z} , S_{C_z} , S_{D_z}), ϕ_{Acolor} (ϕ_{Bcolor} , ϕ_{Ccolor} , ϕ_{Dcolor}), ϕ_{Arel} (ϕ_{Brel} , ϕ_{Crel} , ϕ_{Drel}), and $\chi_{S_A S_{A_z}}$ ($\chi_{S_B S_{B_z}}$, $\chi_{S_C S_{C_z}}$, $\chi_{S_D S_{D_z}}$) are the color wave function, quark-antiquark relative-motion wave function, and spin wave function of meson A (B , C , D), respectively, and $\varphi_{ABflavor}$ ($\varphi_{CDflavor}$) is the flavor wave function of mesons A and B (C and D).

The development in the spherical harmonics of the relative-motion wave function of mesons A and B (aside from a normalization constant) is given by

$$\begin{aligned} e^{i\vec{p}_{q_1\bar{q}_1, q_2\bar{q}_2} \cdot \vec{r}_{q_1\bar{q}_1, q_2\bar{q}_2}} &= 4\pi \sum_{L_1=0}^{\infty} \sum_{M_1=-L_1}^{L_1} i^{L_1} J_{L_1}(|\vec{p}_{q_1\bar{q}_1, q_2\bar{q}_2}| r_{q_1\bar{q}_1, q_2\bar{q}_2}) \\ &\times Y_{L_1 M_1}^*(\hat{p}_{q_1\bar{q}_1, q_2\bar{q}_2}) Y_{L_1 M_1}(\hat{r}_{q_1\bar{q}_1, q_2\bar{q}_2}), \end{aligned} \quad (6)$$

and the development in the spherical harmonics of the relative-motion wave function of mesons C and D leads to

$$e^{-i\vec{p}_{q_3\bar{q}_1,q_2\bar{q}_4}\cdot\vec{r}_{q_3\bar{q}_1,q_2\bar{q}_4}}=4\pi\sum_{L_i=0}^{\infty}\sum_{M_i=-L_i}^{L_i}i^{L_i}(-1)^{L_i}j_{L_i}(|\vec{p}_{q_3\bar{q}_1,q_2\bar{q}_4}|r_{q_3\bar{q}_1,q_2\bar{q}_4})\chi_{S_A S_{A_z} S_B S_{B_z}}=\sum_{S=S_{\min}}^{S_{\max}}\sum_{S_z=-S}^S(S_A S_{A_z} S_B S_{B_z}|S S_z)\chi_{S S_z}, \quad (9)$$

$$\times Y_{L_i M_i}^*(\hat{p}_{q_3\bar{q}_1,q_2\bar{q}_4})Y_{L_i M_i}(\hat{r}_{q_3\bar{q}_1,q_2\bar{q}_4}), \quad (7)$$

$$\chi_{S_C S_{C_z} S_D S_{D_z}}=\sum_{S'=S'_{\min}}^{S'_{\max}}\sum_{S'_z=-S'}^{S'}(S_C S_{C_z} S_D S_{D_z}|S' S'_z)\chi_{S' S'_z}, \quad (10)$$

in $\mathcal{M}_{a\bar{q}_1\bar{q}_2}$, and

$$e^{-i\vec{p}_{q_1\bar{q}_4,q_3\bar{q}_2}\cdot\vec{r}_{q_1\bar{q}_4,q_3\bar{q}_2}}=4\pi\sum_{L_i=0}^{\infty}\sum_{M_i=-L_i}^{L_i}i^{L_i}(-1)^{L_i}j_{L_i}(|\vec{p}_{q_1\bar{q}_4,q_3\bar{q}_2}|r_{q_1\bar{q}_4,q_3\bar{q}_2})\chi_{S_A S_{A_z} S_B S_{B_z}}=\sum_{S=S_{\min}}^{S_{\max}}\sum_{S_z=-S}^S(S_A S_{A_z} S_B S_{B_z}|S S_z)\chi_{S S_z}, \quad (8)$$

$$\times Y_{L_i M_i}^*(\hat{p}_{q_1\bar{q}_4,q_3\bar{q}_2})Y_{L_i M_i}(\hat{r}_{q_1\bar{q}_4,q_3\bar{q}_2}),$$

in $\mathcal{M}_{a\bar{q}_1\bar{q}_2}$, where $Y_{L_i M_i}$ ($Y_{L_i M_i}$) are the spherical harmonics with the orbital-angular-momentum quantum number L_i (L_f) and the magnetic projection quantum number M_i (M_f), j_{L_i} and j_{L_f} are the spherical Bessel functions, and $\hat{p}_{q_1\bar{q}_1,q_2\bar{q}_2}$ ($\hat{p}_{q_3\bar{q}_1,q_2\bar{q}_4}$, $\hat{p}_{q_1\bar{q}_4,q_3\bar{q}_2}$, $\hat{r}_{q_1\bar{q}_1,q_2\bar{q}_2}$, $\hat{r}_{q_3\bar{q}_1,q_2\bar{q}_4}$, $\hat{r}_{q_1\bar{q}_4,q_3\bar{q}_2}$) denotes the polar angles of $\vec{p}_{q_1\bar{q}_1,q_2\bar{q}_2}$ ($\vec{p}_{q_3\bar{q}_1,q_2\bar{q}_4}$, $\vec{p}_{q_1\bar{q}_4,q_3\bar{q}_2}$, $\vec{r}_{q_1\bar{q}_1,q_2\bar{q}_2}$, $\vec{r}_{q_3\bar{q}_1,q_2\bar{q}_4}$, $\vec{r}_{q_1\bar{q}_4,q_3\bar{q}_2}$).

Let χ_{SS_z} ($\chi_{S'S'_z}$) denote the spin wave function of mesons A and B (C and D), which has the total spin S (S') and its z component S_z (S'_z). The Clebsch-Gordan coefficients ($S_A S_{A_z} S_B S_{B_z}|S S_z$) relate χ_{SS_z} to $\chi_{S_A S_{A_z} S_B S_{B_z}}$, and ($S_C S_{C_z} S_D S_{D_z}|S' S'_z$) relate $\chi_{S'S'_z}$ to $\chi_{S_C S_{C_z} S_D S_{D_z}}$.

where $S_{\min}=|S_A-S_B|$, $S_{\max}=S_A+S_B$, $S'_{\min}=|S_C-S_D|$, and $S'_{\max}=S_C+S_D$. $Y_{L_i M_i}$ and χ_{SS_z} ($Y_{L_f M_f}$ and $\chi_{S'S'_z}$) are coupled to the wave function $\varphi_{JJ_z}^{\text{in}}$ ($\varphi_{JJ_z}^{\text{final}}$), which has the total angular momentum J (J') of mesons A and B (C and D) and its z component J_z (J'_z),

$$Y_{L_i M_i} \chi_{SS_z} = \sum_{J=J_{\min}}^{J_{\max}} \sum_{J_z=-J}^J (L_i M_i S S_z | J J_z) \varphi_{JJ_z}^{\text{in}}, \quad (11)$$

$$Y_{L_f M_f} \chi_{S'S'_z} = \sum_{J'=J'_{\min}}^{J'_{\max}} \sum_{J'_z=-J'}^{J'} (L_f M_f S' S'_z | J' J'_z) \varphi_{J'J'_z}^{\text{final}}, \quad (12)$$

where $J_{\min}=|L_i-S|$, $J_{\max}=L_i+S$, $J'_{\min}=|L_f-S'|$, and $J'_{\max}=L_f+S'$. ($L_i M_i S S_z | J J_z$) and ($L_f M_f S' S'_z | J' J'_z$) are the Clebsch-Gordan coefficients. It follows from Eqs. (6)–(12) that the transition amplitude given in Eq. (3) becomes

$$\mathcal{M}_{a\bar{q}_1\bar{q}_2} = \frac{(m_{q_1} + m_{\bar{q}_4})^3}{m_{q_1}^3} \sqrt{2E_A 2E_B 2E_C 2E_D} (4\pi)^2 \sum_{L_i=0}^{\infty} \sum_{M_i=-L_i}^{L_i} i^{L_i} Y_{L_i M_i}^*(\hat{p}_{q_1\bar{q}_1,q_2\bar{q}_2})$$

$$\times \sum_{L_f=0}^{\infty} \sum_{M_f=-L_f}^{L_f} i^{L_f} (-1)^{L_f} Y_{L_f M_f}^*(\hat{p}_{q_1\bar{q}_4,q_3\bar{q}_2}) \phi_{C\text{color}}^+ \phi_{D\text{color}}^+ \phi_{CD\text{flavor}}^+ \int d\vec{r}_{q_1\bar{q}_1} d\vec{r}_{q_3\bar{q}_2} d\vec{r}_{q_1\bar{q}_4,q_3\bar{q}_2} \phi_{C\text{rel}}^+ \phi_{D\text{rel}}^+ \sum_{S'S'_z} (S_C S_{C_z} S_D S_{D_z} | S' S'_z)$$

$$\times \sum_{J'J'_z} (L_f M_f S' S'_z | J' J'_z) \varphi_{J'J'_z}^{\text{final}} V_{a\bar{q}_1\bar{q}_2} \sum_{SS_z} (S_A S_{A_z} S_B S_{B_z} | S S_z) \sum_{JJ_z} (L_i M_i S S_z | J J_z) \varphi_{JJ_z}^{\text{in}} \phi_{A\text{rel}} \phi_{B\text{rel}} \varphi_{AB\text{flavor}} \phi_{A\text{color}} \phi_{B\text{color}}$$

$$\times j_{L_i}(|\vec{p}_{q_1\bar{q}_1,q_2\bar{q}_2}|r_{q_1\bar{q}_1,q_2\bar{q}_2}) j_{L_f}(|\vec{p}_{q_1\bar{q}_4,q_3\bar{q}_2}|r_{q_1\bar{q}_4,q_3\bar{q}_2}). \quad (13)$$

Conservation of the total angular momentum implies that J equals J' and J_z equals J'_z . This leads to

$$\mathcal{M}_{a\bar{q}_1\bar{q}_2} = \frac{(m_{q_1} + m_{\bar{q}_4})^3}{m_{q_1}^3} \sqrt{2E_A 2E_B 2E_C 2E_D} (4\pi)^2 \sum_{L_i=0}^{\infty} \sum_{M_i=-L_i}^{L_i} i^{L_i} Y_{L_i M_i}^*(\hat{p}_{q_1\bar{q}_1,q_2\bar{q}_2})$$

$$\times \sum_{L_f=0}^{\infty} \sum_{M_f=-L_f}^{L_f} i^{L_f} (-1)^{L_f} Y_{L_f M_f}^*(\hat{p}_{q_1\bar{q}_4,q_3\bar{q}_2}) \phi_{C\text{color}}^+ \phi_{D\text{color}}^+ \phi_{CD\text{flavor}}^+ \int d\vec{r}_{q_1\bar{q}_1} d\vec{r}_{q_3\bar{q}_2} d\vec{r}_{q_1\bar{q}_4,q_3\bar{q}_2} \phi_{C\text{rel}}^+ \phi_{D\text{rel}}^+ \sum_{S'S'_z} (S_C S_{C_z} S_D S_{D_z} | S' S'_z)$$

$$\times \sum_{JJ_z} (L_f M_f S' S'_z | J J_z) \varphi_{JJ_z}^{\text{final}} V_{a\bar{q}_1\bar{q}_2} \sum_{SS_z} (S_A S_{A_z} S_B S_{B_z} | S S_z) (L_i M_i S S_z | J J_z) \varphi_{JJ_z}^{\text{in}} \phi_{A\text{rel}} \phi_{B\text{rel}} \varphi_{AB\text{flavor}} \phi_{A\text{color}} \phi_{B\text{color}}$$

$$\times j_{L_i}(|\vec{p}_{q_1\bar{q}_1,q_2\bar{q}_2}|r_{q_1\bar{q}_1,q_2\bar{q}_2}) j_{L_f}(|\vec{p}_{q_1\bar{q}_4,q_3\bar{q}_2}|r_{q_1\bar{q}_4,q_3\bar{q}_2}). \quad (14)$$

Using the relation

$$\varphi_{JJ_z}^{\text{in}} = \sum_{\bar{M}_i \bar{S}_z} (L_i \bar{M}_i S \bar{S}_z | JJ_z) Y_{L_i \bar{M}_i} \chi_{S \bar{S}_z}, \tag{15}$$

$$\varphi_{JJ_z}^{\text{final}} = \sum_{\bar{M}_i \bar{S}_z} (L_f \bar{M}_f S' \bar{S}'_z | JJ_z) Y_{L_f \bar{M}_f} \chi_{S' \bar{S}'_z}, \tag{16}$$

where $(L_i \bar{M}_i S \bar{S}_z | JJ_z)$ and $(L_f \bar{M}_f S' \bar{S}'_z | JJ_z)$ are the Clebsch-Gordan coefficients, we get

$$\begin{aligned} \mathcal{M}_{a\bar{q}_1, q_2} &= \frac{(m_{q_1} + m_{\bar{q}_1})^3}{m_{q_1}^3} \sqrt{2E_A 2E_B 2E_C 2E_D} (4\pi)^2 \sum_{L_i=0}^{\infty} \sum_{M_i=-L_i}^{L_i} i^{L_i} Y_{L_i M_i}^*(\hat{p}_{q_1, \bar{q}_1, q_2, \bar{q}_2}) \\ &\times \sum_{L_f=0}^{\infty} \sum_{M_f=-L_f}^{L_f} i^{L_f} (-1)^{L_f} Y_{L_f M_f}^*(\hat{p}_{q_1, \bar{q}_1, q_3, \bar{q}_2}) \sum_{S' \bar{S}'_z} (S_C S_{C_z} S_D S_{D_z} | S' \bar{S}'_z) \\ &\times \sum_{JJ_z} (L_f \bar{M}_f S' \bar{S}'_z | JJ_z) \sum_{\bar{M}_i \bar{S}_z} (L_f \bar{M}_f S' \bar{S}'_z | JJ_z) \sum_{SS_z} (S_A S_{A_z} S_B S_{B_z} | S S_z) \\ &\times (L_i \bar{M}_i S \bar{S}_z | JJ_z) \sum_{\bar{M}_i \bar{S}_z} (L_i \bar{M}_i S \bar{S}_z | JJ_z) \phi_{C\text{color}}^+ \phi_{D\text{color}}^+ \phi_{CD\text{flavor}}^+ \chi_{S \bar{S}_z}^+ \\ &\times \int d\vec{r}_{q_1, \bar{q}_1} d\vec{r}_{q_3, \bar{q}_2} d\vec{r}_{q_1, \bar{q}_1, q_3, \bar{q}_2} j_{L_i}(|\vec{p}_{q_1, \bar{q}_1, q_3, \bar{q}_2}| r_{q_1, \bar{q}_1, q_3, \bar{q}_2}) Y_{L_i \bar{M}_i}(\hat{r}_{q_1, \bar{q}_1, q_3, \bar{q}_2}) \\ &\times \phi_{C\text{rel}}^+ \phi_{D\text{rel}}^+ V_{a\bar{q}_1, q_2} \phi_{A\text{rel}} \phi_{B\text{rel}} j_{L_f}(|\vec{p}_{q_1, \bar{q}_1, q_2, \bar{q}_2}| r_{q_1, \bar{q}_1, q_2, \bar{q}_2}) Y_{L_f \bar{M}_f}(\hat{r}_{q_1, \bar{q}_1, q_2, \bar{q}_2}) \\ &\times \chi_{S \bar{S}_z} \phi_{AB\text{flavor}} \phi_{A\text{color}} \phi_{B\text{color}}. \end{aligned} \tag{17}$$

Furthermore, we need the identity

$$j_l(pr) Y_{lm}(\hat{r}) = \int \frac{d^3 p'}{(2\pi)^3} \frac{2\pi^2}{p^2} \delta(p - p') i^l (-1)^l Y_{lm}(\hat{p}') e^{i\vec{p}' \cdot \vec{r}}, \tag{18}$$

which is obtained with the help of $\int_0^\infty j_l(pr) j_l(p'r) r^2 dr = \frac{\pi}{2p^2} \delta(p - p')$ [31, 32], and where \hat{r} (\hat{p}') denotes the polar angles of \vec{r} (\vec{p}'). Substituting Eq. (18) in Eq. (17), we get

$$\begin{aligned} \mathcal{M}_{a\bar{q}_1, q_2} &= \frac{(m_{q_1} + m_{\bar{q}_1})^3}{m_{q_1}^3} \sqrt{2E_A 2E_B 2E_C 2E_D} (4\pi)^2 \sum_{L_i=0}^{\infty} \sum_{M_i=-L_i}^{L_i} i^{L_i} Y_{L_i M_i}^*(\hat{p}_{q_1, \bar{q}_1, q_2, \bar{q}_2}) \\ &\times \sum_{L_f=0}^{\infty} \sum_{M_f=-L_f}^{L_f} i^{L_f} (-1)^{L_f} Y_{L_f M_f}^*(\hat{p}_{q_1, \bar{q}_1, q_3, \bar{q}_2}) \sum_{S' \bar{S}'_z} (S_C S_{C_z} S_D S_{D_z} | S' \bar{S}'_z) \\ &\times \sum_{JJ_z} (L_f \bar{M}_f S' \bar{S}'_z | JJ_z) \sum_{\bar{M}_i \bar{S}_z} (L_f \bar{M}_f S' \bar{S}'_z | JJ_z) \sum_{SS_z} (S_A S_{A_z} S_B S_{B_z} | S S_z) \\ &\times (L_i \bar{M}_i S \bar{S}_z | JJ_z) \sum_{\bar{M}_i \bar{S}_z} (L_i \bar{M}_i S \bar{S}_z | JJ_z) \phi_{C\text{color}}^+ \phi_{D\text{color}}^+ \phi_{CD\text{flavor}}^+ \chi_{S \bar{S}_z}^+ \\ &\times \int \frac{d^3 p_{\text{firm}}}{(2\pi)^3} \frac{2\pi^2}{\vec{p}_{q_1, \bar{q}_1, q_3, \bar{q}_2}^2} \delta(|\vec{p}_{q_1, \bar{q}_1, q_3, \bar{q}_2}| - |\vec{p}_{\text{firm}}|) i^{L_i} (-1)^{L_i} Y_{L_i \bar{M}_i}(\hat{p}_{\text{firm}}) \end{aligned}$$

$$\begin{aligned}
 & \times \int \frac{d^3 p_{\text{irm}}}{(2\pi)^3} \frac{2\pi^2}{\vec{p}_{q_1, \bar{q}_1, q_2, \bar{q}_2}^2} \delta(|\vec{p}_{q_1, \bar{q}_1, q_2, \bar{q}_2}| - |\vec{p}_{\text{irm}}|) i^{L_i} (-1)^{L_i} Y_{L_i, \bar{M}_i}(\hat{p}_{\text{irm}}) \\
 & \times \int d\vec{r}_{q_1, \bar{q}_1} d\vec{r}_{q_3, \bar{q}_2} d\vec{r}_{q_1, \bar{q}_4, q_3, \bar{q}_2} \phi_{\text{Crel}}^+ \phi_{\text{Drel}}^+ V_{a\bar{q}_1, q_2} \phi_{\text{Arel}} \phi_{\text{Brel}} \\
 & \times e^{i\vec{p}_{\text{irm}} \cdot \vec{r}_{q_1, \bar{q}_1, q_3, \bar{q}_2}} e^{i\vec{p}_{\text{irm}} \cdot \vec{r}_{q_1, \bar{q}_1, q_2, \bar{q}_2}} \chi_{S\bar{S}_z} \varphi_{AB\text{flavor}} \phi_{\text{Acolor}} \phi_{\text{Bcolor}}. \tag{19}
 \end{aligned}$$

Let \vec{r}_c be the position vector of constituent c . ϕ_{Arel} and ϕ_{Brel} are functions of the relative coordinate of the quark and antiquark inside mesons A and B , respectively. We take the Fourier transform of $V_{a\bar{q}_1, q_2}$, $V_{a\bar{q}_1, q_2}$, ϕ_{Arel} , and ϕ_{Brel} :

$$V_{a\bar{q}_1, q_2}(\vec{r}_{q_3} - \vec{r}_{q_1}) = \int \frac{d^3 k}{(2\pi)^3} V_{a\bar{q}_1, q_2}(\vec{k}) e^{i\vec{k} \cdot (\vec{r}_{q_3} - \vec{r}_{q_1})}, \tag{20}$$

$$V_{a\bar{q}_1, q_2}(\vec{r}_{q_3} - \vec{r}_{q_2}) = \int \frac{d^3 k}{(2\pi)^3} V_{a\bar{q}_1, q_2}(\vec{k}) e^{i\vec{k} \cdot (\vec{r}_{q_3} - \vec{r}_{q_2})}, \tag{21}$$

$$\phi_{\text{Arel}}(\vec{r}_{q_1, \bar{q}_1}) = \int \frac{d^3 p_{q_1, \bar{q}_1}}{(2\pi)^3} \phi_{\text{Arel}}(\vec{p}_{q_1, \bar{q}_1}) e^{i\vec{p}_{q_1, \bar{q}_1} \cdot \vec{r}_{q_1, \bar{q}_1}}, \tag{22}$$

$$\phi_{\text{Brel}}(\vec{r}_{q_2, \bar{q}_2}) = \int \frac{d^3 p_{q_2, \bar{q}_2}}{(2\pi)^3} \phi_{\text{Brel}}(\vec{p}_{q_2, \bar{q}_2}) e^{i\vec{p}_{q_2, \bar{q}_2} \cdot \vec{r}_{q_2, \bar{q}_2}}. \tag{23}$$

In Eqs. (20)–(21), \vec{k} is the gluon momentum, and in Eqs. (22)–(23), \vec{p}_{ab} is the relative momentum of constituents a and b . In momentum space, the normalizations are

$$\int \frac{d^3 p_{q_1, \bar{q}_1}}{(2\pi)^3} \phi_{\text{Arel}}^+(\vec{p}_{q_1, \bar{q}_1}) \phi_{\text{Arel}}(\vec{p}_{q_1, \bar{q}_1}) = 1,$$

$$\int \frac{d^3 p_{q_2, \bar{q}_2}}{(2\pi)^3} \phi_{\text{Brel}}^+(\vec{p}_{q_2, \bar{q}_2}) \phi_{\text{Brel}}(\vec{p}_{q_2, \bar{q}_2}) = 1.$$

The spherical polar coordinates of \vec{p}_{irm} and \vec{p}_{frm} are expressed as $(|\vec{p}_{\text{irm}}|, \theta_{\text{irm}}, \phi_{\text{irm}})$ and $(|\vec{p}_{\text{frm}}|, \theta_{\text{frm}}, \phi_{\text{frm}})$, respectively. Integration over $|\vec{p}_{\text{irm}}|$, $|\vec{p}_{\text{frm}}|$, \vec{r}_{q_1, \bar{q}_1} , \vec{r}_{q_3, \bar{q}_2} , and $\vec{r}_{q_1, \bar{q}_4, q_3, \bar{q}_2}$ in Eq. (19) yields

$$\begin{aligned}
 \mathcal{M}_{a\bar{q}_1, q_2} &= \sqrt{2E_A 2E_B 2E_C 2E_D} \sum_{L_i=0}^{\infty} \sum_{M_i=-L_i}^{L_i} Y_{L_i, M_i}^*(\hat{p}_{q_1, \bar{q}_1, q_2, \bar{q}_2}) \\
 & \times \sum_{L_f=0}^{\infty} \sum_{M_f=-L_f}^{L_f} (-1)^{L_f} Y_{L_f, M_f}^*(\hat{p}_{q_1, \bar{q}_4, q_3, \bar{q}_2}) \sum_{S' S'_z} (S_C S_{C_z} S_D S_{D_z} | S' S'_z) \\
 & \times \sum_{J J_z} (L_f M_f S' S'_z | J J_z) \sum_{\bar{M}_f \bar{S}'_z} (L_f \bar{M}_f S' \bar{S}'_z | J J_z) \sum_{S S_z} (S_A S_{A_z} S_B S_{B_z} | S S_z) \\
 & \times (L_i M_i S S_z | J J_z) \sum_{\bar{M}_i \bar{S}_z} (L_i \bar{M}_i S \bar{S}_z | J J_z) \phi_{\text{Ccolor}}^+ \phi_{\text{Dcolor}}^+ \varphi_{CD\text{flavor}}^+ \chi_{S\bar{S}_z}^+ \\
 & \times \int d\theta_{\text{frm}} d\phi_{\text{frm}} \sin \theta_{\text{frm}} Y_{L_i, \bar{M}_i}(\hat{p}_{\text{frm}}) \int d\theta_{\text{irm}} d\phi_{\text{irm}} \sin \theta_{\text{irm}} Y_{L_i, \bar{M}_i}(\hat{p}_{\text{irm}}) \\
 & \times \int \frac{d^3 p_{q_1, \bar{q}_1}}{(2\pi)^3} \int \frac{d^3 p_{q_2, \bar{q}_2}}{(2\pi)^3} \phi_{\text{Crel}}^+(\vec{p}_{q_1, \bar{q}_1} + \frac{m_{q_1}}{m_{q_1} + m_{\bar{q}_1}} \vec{p}_{\text{irm}} + \frac{m_{q_1}}{m_{q_1} + m_{\bar{q}_4}} \vec{p}_{\text{frm}}) \\
 & \times \phi_{\text{Drel}}^+(\vec{p}_{q_2, \bar{q}_2} + \frac{m_{\bar{q}_2}}{m_{q_2} + m_{\bar{q}_2}} \vec{p}_{\text{irm}} + \frac{m_{\bar{q}_2}}{m_{q_3} + m_{\bar{q}_2}} \vec{p}_{\text{frm}}) \\
 & \times V_{a\bar{q}_1, q_2}[\vec{p}_{q_2, \bar{q}_2} - \vec{p}_{q_1, \bar{q}_1} - (\frac{m_{q_2}}{m_{q_2} + m_{\bar{q}_2}} - \frac{m_{\bar{q}_1}}{m_{q_1} + m_{\bar{q}_1}}) \vec{p}_{\text{irm}}] \\
 & \times \phi_{\text{Arel}}(\vec{p}_{q_1, \bar{q}_1}) \phi_{\text{Brel}}(\vec{p}_{q_2, \bar{q}_2}) \chi_{S\bar{S}_z} \varphi_{AB\text{flavor}} \phi_{\text{Acolor}} \phi_{\text{Bcolor}}, \tag{24}
 \end{aligned}$$

in which $|\vec{p}_{\text{irm}}| = |\vec{p}_{q_1, \bar{q}_1, q_2, \bar{q}_2}|$ and $|\vec{p}_{\text{frm}}| = |\vec{p}_{q_1, \bar{q}_4, q_3, \bar{q}_2}|$, \hat{p}_{irm} (\hat{p}_{frm}) denotes the polar angles of \vec{p}_{irm} (\vec{p}_{frm}), and m_{q_2} and $m_{\bar{q}_2}$ are the q_2 and \bar{q}_2 masses, respectively. The expression for the other transition amplitude $\mathcal{M}_{a\bar{q}_1, \bar{q}_2}$ is similar to

the right-hand side in Eq. (24) and is thus given from $\mathcal{M}_{a\bar{q}_1, q_2}$ by replacing $\hat{p}_{q_1, \bar{q}_4, q_3, \bar{q}_2}$ ($\vec{p}_{q_1, \bar{q}_1} + \frac{m_{q_1}}{m_{q_1} + m_{\bar{q}_1}} \vec{p}_{\text{irm}} + \frac{m_{q_1}}{m_{q_1} + m_{\bar{q}_4}} \vec{p}_{\text{frm}}$, $\vec{p}_{q_2, \bar{q}_2} + \frac{m_{\bar{q}_2}}{m_{q_2} + m_{\bar{q}_2}} \vec{p}_{\text{irm}} + \frac{m_{\bar{q}_2}}{m_{q_3} + m_{\bar{q}_2}} \vec{p}_{\text{frm}}$, $\vec{p}_{q_2, \bar{q}_2} - \vec{p}_{q_1, \bar{q}_1} -$

$(\frac{m_{q_2}}{m_{q_1}+m_{q_2}} - \frac{m_{\bar{q}_1}}{m_{q_1}+m_{\bar{q}_1}})\vec{P}'_{\text{irm}}$ with $\hat{P}_{q_3\bar{q}_1,q_2\bar{q}_4}(\vec{P}_{q_1\bar{q}_1} - \frac{m_{\bar{q}_1}}{m_{q_1}+m_{\bar{q}_1}}\vec{P}'_{\text{irm}} - \frac{m_{q_2}}{m_{q_1}+m_{q_2}}\vec{P}'_{\text{irm}}, \vec{P}_{q_2\bar{q}_2} - \frac{m_{q_2}}{m_{q_2}+m_{\bar{q}_2}}\vec{P}'_{\text{irm}} - \frac{m_{q_2}}{m_{q_2}+m_{q_4}}\vec{P}'_{\text{irm}}, \vec{P}_{q_1\bar{q}_1} - \vec{P}_{q_2\bar{q}_2} + (\frac{m_{q_1}}{m_{q_1}+m_{q_1}} - \frac{m_{q_2}}{m_{q_2}+m_{q_2}})\vec{P}'_{\text{irm}})$. Thus far, we have obtained new expressions for the transition amplitudes from Eqs. (2) and (3).

With the transition amplitudes, the unpolarized cross section for $A + B \rightarrow C + D$ is

$$\begin{aligned}
 \sigma^{\text{unpol}}(\sqrt{s}, T) &= \frac{1}{(2J_A + 1)(2J_B + 1)} \frac{1}{32\pi s} \frac{|\vec{P}'(\sqrt{s})|}{|\vec{P}(\sqrt{s})|} \\
 &\times \int_0^\pi d\theta \sum_{J_{A_z} J_{B_z} J_{C_z} J_{D_z}} |\mathcal{M}_{a q_1 \bar{q}_2} + \mathcal{M}_{a \bar{q}_1 q_2}|^2 \sin\theta,
 \end{aligned} \quad (25)$$

where s is the Mandelstam variable obtained from the four-momenta P_A and P_B of mesons A and B using $s = (P_A + P_B)^2$, T is the temperature, J_A (J_B , J_C , J_D) and J_{A_z} (J_{B_z} , J_{C_z} , J_{D_z}) of meson A (B , C , D) are the total angular momentum and its z component, respectively, θ is the angle between \vec{P} and \vec{P}' , which are the three-dimensional momenta of mesons A and C in the center-of-mass frame, respectively. Let m_A , m_B , m_C , and m_D be the masses of mesons A , B , C , and D , respectively. \vec{P} and \vec{P}' are given by

$$\vec{P}^2(\sqrt{s}) = \frac{1}{4s} [(s - m_A^2 - m_B^2)^2 - 4m_A^2 m_B^2], \quad (26)$$

$$\vec{P}'^2(\sqrt{s}) = \frac{1}{4s} [(s - m_C^2 - m_D^2)^2 - 4m_C^2 m_D^2]. \quad (27)$$

Based on the relativistic energy-momentum relation, we have

$$E_A = \sqrt{\vec{P}^2 + m_A^2} = \frac{1}{2\sqrt{s}}(s + m_A^2 - m_B^2), \quad (28)$$

$$E_B = \sqrt{\vec{P}^2 + m_B^2} = \frac{1}{2\sqrt{s}}(s - m_A^2 + m_B^2), \quad (29)$$

$$E_C = \sqrt{\vec{P}'^2 + m_C^2} = \frac{1}{2\sqrt{s}}(s + m_C^2 - m_D^2), \quad (30)$$

$$E_D = \sqrt{\vec{P}'^2 + m_D^2} = \frac{1}{2\sqrt{s}}(s - m_C^2 + m_D^2). \quad (31)$$

We calculate the cross section in the center-of-mass frame of the two initial mesons. According to the Feynman rules, the two processes $q_1 + \bar{q}_2 \rightarrow q_3 + \bar{q}_4$ and $\bar{q}_1 + q_2 \rightarrow q_3 + \bar{q}_4$ contribute to meson-meson scattering on an equal footing, and the sum $\mathcal{M}_{a q_1 \bar{q}_2} + \mathcal{M}_{a \bar{q}_1 q_2}$ appears in Eq. (25) if $\mathcal{M}_{a q_1 \bar{q}_2} \neq 0$ and $\mathcal{M}_{a \bar{q}_1 q_2} \neq 0$.

III. NUMERICAL CROSS SECTIONS AND DISCUSSIONS

The quark-antiquark relative-motion wave functions $\phi_{A\text{rel}}$ and $\phi_{B\text{rel}}$ in Eq. (4) as well as $\phi_{C\text{rel}}$ and $\phi_{D\text{rel}}$ in Eq. (5) are solutions of the Schrödinger equation with a temperature-dependent quark potential. The potential between constituents a and b in coordinate space is [29]

$$\begin{aligned}
 V_{ab}(\vec{r}_{ab}) &= -\frac{\vec{\lambda}_a}{2} \cdot \frac{\vec{\lambda}_b}{2} \xi_1 \left[1.3 - \left(\frac{T}{T_c} \right)^4 \right] \tanh(\xi_2 r_{ab}) \\
 &+ \frac{\vec{\lambda}_a}{2} \cdot \frac{\vec{\lambda}_b}{2} \frac{6\pi v(\lambda r_{ab})}{25 r_{ab}} \exp(-\xi_3 r_{ab}) \\
 &- \frac{\vec{\lambda}_a}{2} \cdot \frac{\vec{\lambda}_b}{2} \frac{16\pi^2 d^3}{25 \pi^{3/2}} \exp(-d^2 r_{ab}^2) \frac{\vec{s}_a \cdot \vec{s}_b}{m_a m_b} \\
 &+ \frac{\vec{\lambda}_a}{2} \cdot \frac{\vec{\lambda}_b}{2} \frac{4\pi}{25 r_{ab}} \frac{1}{dr_{ab}^2} \frac{d^2 v(\lambda r_{ab})}{dr_{ab}^2} \frac{\vec{s}_a \cdot \vec{s}_b}{m_a m_b},
 \end{aligned} \quad (32)$$

where $\xi_1 = 0.525$ GeV, $\xi_2 = 1.5[0.75 + 0.25(T/T_c)^{10}]^6$ GeV, $\xi_3 = 0.6$ GeV, and $\lambda = \sqrt{25/16\pi^2 \alpha'}$ with $\alpha' = 1.04$ GeV⁻², $T_c = 0.175$ GeV is the critical temperature at which the phase transition between quark-gluon plasma and hadronic matter takes place [33–35], m_a , \vec{s}_a , and $\vec{\lambda}_a$ are the mass, spin, and Gell-Mann matrices for the color generators of constituent a , respectively, the dimensionless function v is given by Buchmüller and Tye in Ref. [36], and the quantity d is related to constituent quark masses via

$$d^2 = d_1^2 \left[\frac{1}{2} + \frac{1}{2} \left(\frac{4m_a m_b}{(m_a + m_b)^2} \right)^4 \right] + d_2^2 \left(\frac{2m_a m_b}{m_a + m_b} \right)^2, \quad (33)$$

where $d_1 = 0.15$ GeV and $d_2 = 0.705$. The potential originates from perturbative quantum chromodynamics (QCD) at short distances and lattice QCD at intermediate and long distances. The first and second terms are the central spin-independent potential of which the short-distance part arises from one-gluon exchange plus perturbative one- and two-loop corrections in vacuum [36] and the intermediate-distance and long-distance part effectively fits the numerical potential, which was obtained in lattice gauge calculations [33]. The third term is the smeared spin-spin interaction that originates from one-gluon exchange between constituents a and b [37], and the fourth term is the spin-spin interaction that arises from perturbative one- and two-loop corrections to one-gluon exchange [38]. The temperature dependence of the potential is given by the first term and originates from the lattice gauge calculations [33]. At long distances, the spin-independent potential is independent of r_{ab} and obviously exhibits a plateau at $T/T_c > 0.55$. The plateau

height decreases with increasing temperature. Thus, confinement becomes progressively weaker.

The Schrödinger equation with the potential yields energy eigenvalues and quark-antiquark relative-motion wave functions in the coordinate space. The sum of the quark mass, antiquark mass, and an energy eigenvalue gives the meson mass. In this study, we use the constituent quark masses 0.32 GeV for the up and down quarks and 0.5 GeV for the strange quark. The quark masses are independent of temperature. The experimental masses of the π , ρ , K , K^* , η , ω , and ϕ mesons are reproduced from the Schrödinger equation with the potential at $T = 0$. Furthermore, the temperature dependence of the potential leads to the temperature dependence of meson masses and mesonic quark-antiquark relative-motion wave functions. The temperature dependence of the π , ρ , K , and K^* masses is shown in Ref. [39], where the temperature covers the temperature region of hadronic matter, and the parameterizations of these meson masses are given. The temperature dependence of the ϕ mass is shown in Ref. [40], which is parameterized as

$$m_\phi = 0.931 \left[1 - \left(\frac{T}{1.12T_c} \right)^{5.46} \right]^{1.32}. \quad (34)$$

Because confinement becomes progressively weaker with increasing temperature, the spatial extension of the mesonic quark-antiquark relative-motion wave functions becomes progressively larger. Because the orbital-angular-momentum quantum numbers of the π , ρ , K , K^* , η , ω , and ϕ mesons are zero, the wave functions are not zero at $r_{ab} = 0$. When the temperature increases, the absolute values of the wave functions at $r_{ab} = 0$ decrease.

The transition potentials $V_{aq_1\bar{q}_2}$ and $V_{a\bar{q}_1q_2}$ are derived from the perturbative QCD in Ref. [29]. From the wave functions and transition potentials, we get the transition amplitudes $\mathcal{M}_{aq_1\bar{q}_2}$ and $\mathcal{M}_{a\bar{q}_1q_2}$. In practical calculations, the summations over L_i and L_f in the transition amplitudes are from 0 to 3. The orbital-angular-momentum quantum numbers L_i and L_f are selected such that parity is conserved and that the total angular momentum of the two final mesons equals the total angular momentum of the two initial mesons. The values of L_i and L_f are listed in Table 1.

We consider the four $K+\phi$ reactions $K\phi \rightarrow \pi K$, $K\phi \rightarrow \rho K$, $K\phi \rightarrow \pi K^*$, and $K\phi \rightarrow \rho K^*$. $\mathcal{M}_{aq_1\bar{q}_2}$ and $\mathcal{M}_{a\bar{q}_1q_2}$ are proportional to flavor matrix elements. Because the flavor matrix elements for the $K+\phi$ reactions with total isospin $I = \frac{1}{2}$ are zero for $\mathcal{M}_{aq_1\bar{q}_2}$ and $-\frac{\sqrt{6}}{2}$ for $\mathcal{M}_{a\bar{q}_1q_2}$, only the process $\bar{q}_1 + q_2 \rightarrow q_3 + \bar{q}_4$ contributes to these reactions. The unpolarized cross section for the four $K+\phi$ reactions is

Table 1. Total spin and orbital-angular-momentum quantum number.

Reaction	S	S'	L_i	L_f
$K\phi \rightarrow \pi K$	1	0	1	1
	1	0	2	2
	1	0	3	3
$K\phi \rightarrow \rho K$	1	1	0	0,2
	1	1	1	1,3
	1	1	2	0,2
	1	1	3	1,3
	1	1	3	1,3
$K\phi \rightarrow \pi K^*$	1	1	0	0,2
	1	1	1	1,3
	1	1	2	0,2
	1	1	3	1,3
	1	1	3	1,3
$K\phi \rightarrow \rho K^*$	1	0	1	1
	1	0	2	2
	1	0	3	3
	1	1	0	0,2
	1	1	1	1,3
	1	1	2	0,2
	1	1	3	1,3
	1	2	0	2
	1	2	1	1,3
	1	2	2	0,2
1	2	3	1,3	

$$\sigma^{\text{unpol}}(\sqrt{s}, T) = \frac{1}{(2J_A + 1)(2J_B + 1)} \frac{1}{32\pi s} \frac{|\vec{P}'(\sqrt{s})|}{|\vec{P}(\sqrt{s})|} \times \int_0^\pi d\theta \sum_{J_{A_c} J_{B_c} J_{C_c} J_{D_c}} |\mathcal{M}_{a\bar{q}_1q_2}|^2 \sin\theta. \quad (35)$$

If the sum of the masses of the two initial mesons of a reaction is larger than that of the two final mesons, the reaction is exothermic. Even slowly-moving initial mesons may start the reaction, and a certain amount of the initial meson masses are converted into the kinetic energies of the final mesons. If the sum of the masses of the two initial mesons is smaller than that of the two final mesons, the reaction is endothermic. The initial mesons need kinetic energies to satisfy energy conservation and to start the reaction, and a certain amount of the kinetic energies are converted into the masses of the final mesons.

The reaction $K\phi \rightarrow \rho K^*$ is endothermic at $T/T_c = 0$ and exothermic at $T/T_c = 0.65, 0.75, 0.85, 0.9, \text{ and } 0.95$. The other three reactions are exothermic. The cross sections for exothermic reactions are infinite at threshold energies. Thus, we begin cross section calculations for exo-

thermic reactions at $\sqrt{s} = m_K + m_\phi + 10^{-4}$ GeV, where m_K and m_ϕ are the masses of the kaon and ϕ meson, respectively. Numerical unpolarized cross sections for $K\phi \rightarrow \pi K$, $K\phi \rightarrow \rho K$, $K\phi \rightarrow \pi K^*$, and $K\phi \rightarrow \rho K^*$ are plotted as red solid curves in Figs. 1 to 4. Because the quark potential, meson masses, and mesonic quark-antiquark relative-motion wave functions depend on the temperature, $|\vec{P}|$, $|\vec{P}'|$, E_A , E_B , E_C , E_D , and $M_{a\bar{q},q_2}$, which are given in Eq. (24) and Eqs. (26)–(31), depend on the temperature. This leads to the temperature dependence of the unpolarized cross sections.

The numerical cross sections for endothermic reactions are parameterized as

$$\begin{aligned} \sigma^{\text{unpol}}(\sqrt{s}, T) = & a_1 \left(\frac{\sqrt{s} - \sqrt{s_0}}{b_1} \right)^{c_1} \\ & \times \exp \left[c_1 \left(1 - \frac{\sqrt{s} - \sqrt{s_0}}{b_1} \right) \right] \\ & + a_2 \left(\frac{\sqrt{s} - \sqrt{s_0}}{b_2} \right)^{c_2} \\ & \times \exp \left[c_2 \left(1 - \frac{\sqrt{s} - \sqrt{s_0}}{b_2} \right) \right], \quad (36) \end{aligned}$$

where $\sqrt{s_0}$ is the threshold energy, and a_1 , b_1 , c_1 , a_2 , b_2 , and c_2 are parameters. The numerical cross sections for exothermic reactions are parameterized as

$$\begin{aligned} \sigma^{\text{unpol}}(\sqrt{s}, T) = & \frac{\vec{P}'^2}{\vec{P}^2} \left\{ a_1 \left(\frac{\sqrt{s} - \sqrt{s_0}}{b_1} \right)^{c_1} \right. \\ & \times \exp \left[c_1 \left(1 - \frac{\sqrt{s} - \sqrt{s_0}}{b_1} \right) \right] \\ & + a_2 \left(\frac{\sqrt{s} - \sqrt{s_0}}{b_2} \right)^{c_2} \\ & \left. \times \exp \left[c_2 \left(1 - \frac{\sqrt{s} - \sqrt{s_0}}{b_2} \right) \right] \right\}. \quad (37) \end{aligned}$$

The parameter values are listed in Table 2. d_0 is the separation between the peak's location on the \sqrt{s} -axis and the threshold energy, and $\sqrt{s_z}$ is the square root of the Mandelstam variable at which the cross section is 1/100 of the peak cross section. For the endothermic reaction $K\phi \rightarrow \rho K^*$ at $T = 0$, a peak is displayed in Fig. 4, and $d_0 = 0.25$ GeV and $\sqrt{s_z} = 3.04$ GeV are obtained from the numerical cross section for $K\phi \rightarrow \rho K^*$. Peak cross sections may not be observed for exothermic reactions; however, \vec{P}^2/\vec{P}'^2 times numerical cross sections must reveal peak cross sections for exothermic reactions. Hence, for exothermic reactions, d_0 and $\sqrt{s_z}$ are obtained from \vec{P}^2/\vec{P}'^2 times the numerical cross sections.

The cross sections given by the parameterizations are plotted as green dashed curves in Figs. 1 to 4. For the exothermic reactions, the solid and dashed curves appear

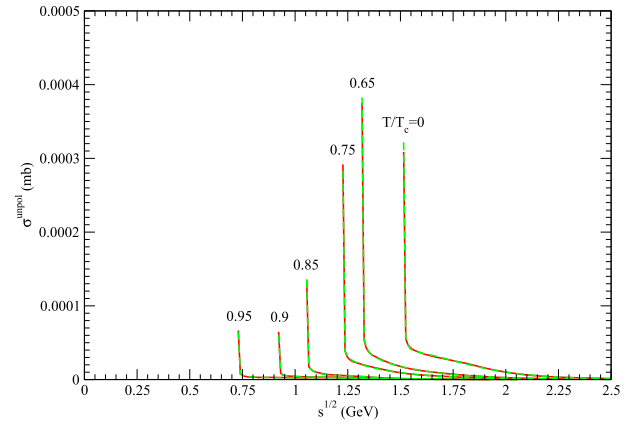


Fig. 1. (color online) Cross sections for $K\phi \rightarrow \pi K$ at various temperatures. The red solid curves and green dashed curves are obtained from Eqs. (35) and (37), respectively.

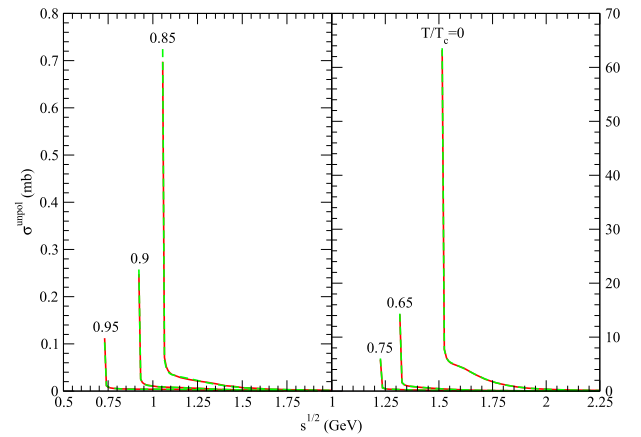


Fig. 2. (color online) Same as Fig. 1 except for $K\phi \rightarrow \rho K$.

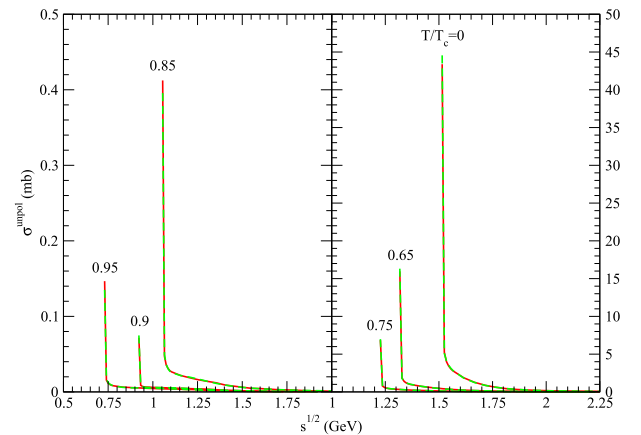


Fig. 3. (color online) Same as Fig. 1 except for $K\phi \rightarrow \pi K^*$.

to coincide. For the endothermic reaction $K\phi \rightarrow \rho K^*$ at $T = 0$, a difference between the solid and dashed curves exists around the two peak cross sections and at $\sqrt{s} > 2.2$ GeV.

The threshold energy for each of the exothermic reactions $K\phi \rightarrow \pi K$, $K\phi \rightarrow \rho K$, and $K\phi \rightarrow \pi K^*$ is the sum of

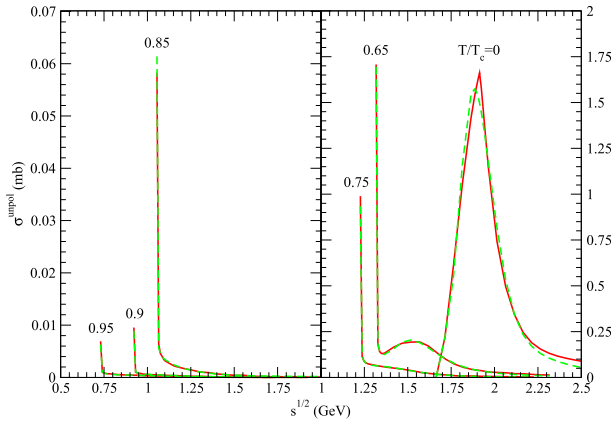


Fig. 4. (color online) Cross sections for $K\phi \rightarrow \rho K^*$ at various temperatures. The red solid curves and green dashed curves are obtained from Eq. (35) and Eqs. (36)–(37), respectively.

the K and ϕ masses. When the temperature increases, the decreases in the masses lead to a decrease in the threshold

energy, as shown in Figs. 1–3. As \sqrt{s} increases near the threshold energy, the cross sections for these reactions decrease rapidly owing to the factor $|\vec{P}'|/|\vec{P}|$ in Eq. (35). The threshold energy of the endothermic reaction $K\phi \rightarrow \rho K^*$ at $T = 0$ is the sum of the ρ and K^* masses. As \sqrt{s} increases from the threshold energy, the cross section for $K\phi \rightarrow \rho K^*$ at $T = 0$ increases rapidly from zero, reaches a peak value of approximately 1.66 mb, and then decreases.

Because the reactions $K\phi \rightarrow \pi K$, $K\phi \rightarrow \rho K$, and $K\phi \rightarrow \pi K^*$ are exothermic, the exclusive final states πK , ρK , and πK^* can always be found in a $K + \phi$ reaction. However, the exclusive final state ρK^* may not be found in a $K + \phi$ reaction in vacuum because the reaction $K\phi \rightarrow \rho K^*$ is endothermic at $T = 0$. If the total energy \sqrt{s} of the K and ϕ mesons in the center-of-mass frame is smaller than the threshold energy of $K\phi \rightarrow \rho K^*$, the reaction does not occur. If \sqrt{s} is larger than the threshold energy, ρK^* production can be observed.

In hadronic matter with high temperatures, the four

Table 2. Values of the parameters. a_1 and a_2 are in units of millibarns, b_1 , b_2 , d_0 , and $\sqrt{s_z}$ are in units of GeV, c_1 and c_2 are dimensionless.

Reaction	T/T_c	a_1	b_1	c_1	a_2	b_2	c_2	d_0	$\sqrt{s_z}$
$K\phi \rightarrow \pi K$	0	0.0000026	0.17	0.62	0.0000046	0.27	1.95	0.3	2.83
	0.65	0.000002	0.13	0.54	0.000003	0.24	1.2	0.15	2.57
	0.75	0.0000002	0.1	0.25	0.0000037	0.19	0.86	0.2	2.46
	0.85	0.00000076	0.239	8.37	0.00000124	0.136	0.58	0.2	2.15
	0.9	0.00000042	0.271	4.7	0.00000094	0.237	0.59	0.3	1.97
	0.95	0.0000008	0.43	5.9	0.0000009	0.23	0.55	0.45	2.17
$K\phi \rightarrow \rho K$	0	0.64	0.125	2.21	0.6	0.107	0.53	0.1	2.87
	0.65	0.11	0.12	0.52	0.07	0.14	2.15	0.15	2.65
	0.75	0.04	0.137	0.49	0.03	0.148	1.93	0.15	1.4
	0.85	0.004	0.183	2.54	0.005	0.167	0.48	0.25	2.81
	0.9	0.00233	0.202	0.5	0.00115	0.2582	4.2	0.25	2.2
	0.95	0.0009	0.371	6.63	0.0014	0.258	0.53	0.4	3.52
$K\phi \rightarrow \pi K^*$	0	0.1	0.153	0.34	0.33	0.096	0.95	0.1	2.94
	0.65	0.121	0.132	0.51	0.068	0.121	1.84	0.15	2.69
	0.75	0.05	0.147	0.5	0.027	0.127	1.65	0.15	2.52
	0.85	0.0025	0.2	3.4	0.0044	0.18	0.55	0.2	2.14
	0.9	0.00089	0.211	0.54	0.00145	0.256	2.24	0.35	2.27
	0.95	0.0014	0.358	3.9	0.0016	0.153	0.55	0.3	1.86
$K\phi \rightarrow \rho K^*$	0	0.29	0.17	0.72	1.29	0.22	6.18	0.25	3.04
	0.65	0.062	0.14	0.49	0.096	0.226	3.9	0.25	4.19
	0.75	0.013	0.202	3.04	0.019	0.123	0.55	0.2	2.48
	0.85	0.00018	0.34	0.28	0.00059	0.11	0.91	0.15	2.16
	0.9	0.000087	0.199	1.86	0.000105	0.153	0.54	0.25	1.48
	0.95	0.00007	0.26	2.7	0.00013	0.17	0.62	0.2	18.02

reactions considered in this study are exothermic and always take place. The K and ϕ mesons satisfy the Bose-Einstein distribution functions. The reactions and distribution reduce the ϕ number and affect the ϕ momentum spectra and ϕ nuclear modification factor, which are observed in ultrarelativistic heavy-ion collisions [3, 6, 13].

The total spin of the two initial mesons in the reaction $K\phi \rightarrow \pi K$ is 1, and the total spin of the two final mesons is 0. Because the two total spins are unequal, the cross section for $K\phi \rightarrow \pi K$ is small. For $K\phi \rightarrow \rho K$, $K\phi \rightarrow \pi K^*$, and $K\phi \rightarrow \rho K^*$, the total spin of the two initial mesons may equal that of the two final mesons, and the cross sections may be a few millibarns when \sqrt{s} is not at the threshold energy.

IV. SUMMARY

With the development in the spherical harmonics of

the relative-motion wave functions of the two initial mesons and two final mesons, new expressions are obtained for the transition amplitudes. With the transition amplitudes, we calculate unpolarized cross sections for $K\phi \rightarrow \pi K$, $K\phi \rightarrow \rho K$, $K\phi \rightarrow \pi K^*$, and $K\phi \rightarrow \rho K^*$, which are governed by quark-antiquark annihilation and creation. Both parity conservation and total-angular-momentum conservation are maintained. To use the numerical cross sections conveniently, we parameterize the cross sections. Each of the exothermic reactions $K\phi \rightarrow \pi K$, $K\phi \rightarrow \rho K$, and $K\phi \rightarrow \pi K^*$ first exhibits a rapid decrease and then a slow decrease in cross section with increasing \sqrt{s} from the threshold energy. Whether the reaction $K\phi \rightarrow \rho K^*$ is endothermic or exothermic depends on temperature. The temperature-dependent cross sections are related to the temperature dependence of the quark potential, quark-antiquark relative-motion wave functions, and meson masses.

References

- [1] J. Rafelski and B. Müller, *Phys. Rev. Lett.* **48**, 1066 (1982)
- [2] A. Shor, *Phys. Rev. Lett.* **54**, 1122 (1985)
- [3] B. I. Abelev *et al.*, *Phys. Rev. Lett.* **99**, 112301 (2007)
- [4] B. I. Abelev *et al.*, *Phys. Lett. B* **673**, 183 (2009)
- [5] B. I. Abelev *et al.*, *Phys. Rev. C* **79**, 064903 (2009)
- [6] A. Adare *et al.*, *Phys. Rev. C* **83**, 024909 (2011)
- [7] L. Adamczyk *et al.*, *Phys. Rev. C* **88**, 014902 (2013)
- [8] L. Adamczyk *et al.*, *Phys. Rev. C* **93**, 021903 (2016)
- [9] J. Adam *et al.*, *Phys. Rev. C* **102**, 034909 (2020)
- [10] M. S. Abdallah *et al.*, *Phys. Rev. C* **105**, 064911 (2022)
- [11] N. J. Abdulameer *et al.*, *Phys. Rev. C* **107**, 014907 (2023)
- [12] B. Abelev *et al.*, *Phys. Rev. C* **91**, 024609 (2015)
- [13] J. Adam *et al.*, *Phys. Rev. C* **95**, 064606 (2017)
- [14] S. Acharya *et al.*, *Phys. Lett. B* **802**, 135225 (2020)
- [15] S. Acharya *et al.*, *Phys. Rev. C* **106**, 034907 (2022)
- [16] P.-Z. Bi and J. Rafelski, *Phys. Lett. B* **262**, 485 (1991)
- [17] C. M. Ko and D. Seibert, *Phys. Rev. C* **49**, 2198 (1994)
- [18] K. Haglin, *Nucl. Phys. A* **584**, 719 (1995)
- [19] W. Smith and K. L. Haglin, *Phys. Rev. C* **57**, 1449 (1998)
- [20] W. S. Chung, G. Q. Li, and C. M. Ko, *Nucl. Phys. A* **625**, 347 (1997)
- [21] L. Alvarez-Ruso and V. Koch, *Phys. Rev. C* **65**, 054901 (2002)
- [22] A. Martínez Torres, K. P. Khemchandani, L. M. Abreu *et al.*, *Phys. Rev. D* **97**, 056001 (2018)
- [23] Z.-F. Luo and X.-M. Xu, *Chin. Phys. C* **36**, 836 (2012)
- [24] X.-M. Xu and H. J. Weber, *Mod. Phys. Lett. A* **35**(33), 2030016 (2020)
- [25] X. Qian *et al.* (CLAS Collaboration), *Phys. Lett. B* **680**, 417 (2009)
- [26] J. Adamczewski-Musch *et al.*, *Phys. Rev. Lett.* **123**, 022002 (2019)
- [27] T. Barnes and E. S. Swanson, *Phys. Rev. D* **46**, 131 (1992)
- [28] E. S. Swanson, *Ann. Phys. (N.Y.)* **220**, 73 (1992)
- [29] Z.-Y. Shen, X.-M. Xu, and H. J. Weber, *Phys. Rev. D* **94**, 034030 (2016)
- [30] T.-T. Wang and X.-M. Xu, *Chin. Phys. C* **43**, 024102 (2019)
- [31] G. B. Arfken and H. J. Weber, *Mathematical Methods for Physicists* (Elsevier, Amsterdam, 2006)
- [32] C. J. Joachain, *Quantum Collision Theory* (North-Holland Publishing Company, Amsterdam, 1983)
- [33] F. Karsch, E. Laermann, and A. Peikert, *Nucl. Phys. B* **605**, 579 (2001)
- [34] S. Dital, P. Petreczky, and H. Satz, *Phys. Lett. B* **514**, 57 (2001)
- [35] X.-M. Xu, C.-Y. Wong, and T. Barnes, *Phys. Rev. C* **67**, 014907 (2003)
- [36] W. Buchmüller and S.-H. H. Tye, *Phys. Rev. D* **24**, 132 (1981)
- [37] S. Godfrey and N. Isgur, *Phys. Rev. D* **32**, 189 (1985)
- [38] X.-M. Xu, *Nucl. Phys. A* **697**, 825 (2002)
- [39] Z.-Y. Shen and X.-M. Xu, *J. Korean Phys. Soc.* **66**, 754 (2015)
- [40] W.-X. Li, X.-M. Xu, and H. J. Weber, *Eur. Phys. J. C* **81**, 225 (2021)